

Victor Prost

GEAR Laboratory,
Department of Mechanical Engineering,
Massachusetts Institute of Technology,
Cambridge, MA 02139
e-mail: vprost@mit.edu

Kathryn M. Olesnavage

GEAR Laboratory,
Department of Mechanical Engineering,
Massachusetts Institute of Technology,
Cambridge, MA 02139
e-mail: kolesnav@mit.edu

W. Brett Johnson

GEAR Laboratory,
Department of Mechanical Engineering,
Massachusetts Institute of Technology,
Cambridge, MA 02139
e-mail: wbj@mit.edu

Matthew J. Major

Professor
Department of Physical Medicine
and Rehabilitation,
Jesse Brown VA Medical Center,
Northwestern University,
Chicago, IL 60208
e-mail: matthew-major@northwestern.edu

Amos G. Winter V

GEAR Laboratory,
Department of Mechanical Engineering,
Massachusetts Institute of Technology,
Cambridge, MA 02139
e-mail: awinter@mit.edu

Design and Testing of a Prosthetic Foot With Interchangeable Custom Springs for Evaluating Lower Leg Trajectory Error, an Optimization Metric for Prosthetic Feet

An experimental prosthetic foot intended for evaluating a novel design objective is presented. This objective, called the lower leg trajectory error (LLTE), enables the optimization of passive prosthetic feet by modeling the trajectory of the shank during single support for a given prosthetic foot and selecting design variables that minimize the error between this trajectory and able-bodied kinematics. A light-weight, fully characterized test foot with variable ankle joint stiffness was designed to evaluate the LLTE. The test foot can replicate the range of motion of a physiological ankle over a range of different ankle joint stiffnesses. The test foot consists of a rotational ankle joint machined from acetel resin, interchangeable U-shaped nylon springs that range from 1.5 N·m/deg to 24 N·m/deg, and a flexible nylon forefoot with a bending stiffness of 16 N·m². The U-shaped springs were designed to support a constant moment along their length to maximize strain energy density; this feature was critical in creating a high-stiffness and high-range of motion ankle. The design performed as predicted during mechanical and in vivo testing, and its modularity allowed us to rapidly vary the ankle joint stiffness. Qualitative feedback from preliminary testing showed that this design is ready for use in large scale clinical trials to further evaluate the use of the LLTE as an optimization objective for passive prosthetic feet. [DOI: 10.1115/1.4039342]

Keywords: compliant mechanisms, mechanism design, prosthetics

1 Introduction

The lower leg trajectory error (LLTE) is a novel optimization metric that can be used to design passive prosthetic feet tailored to a subject's body mass and size. This novel metric, proposed by the authors in previous work [1], relates the mechanical attributes of a passive foot to the gait of an amputee. It involves modeling the trajectory of the lower leg segment (shank) throughout the single support phase of gait for a given prosthetic foot. The lower leg trajectory in the sagittal plane can be described by three variables:

x_{knee} , y_{knee} , and θ_{LL} . To compute the LLTE, these variables are compared to target physiological values taken from published gait data [2], \hat{x}_{knee} , \hat{y}_{knee} , and $\hat{\theta}_{LL}$. These variables are a set of discrete points taken at different time intervals. The normalization of the root-mean-square error was chosen to reduce the bias toward any of the kinematic variables and was done by using the average values of each of the physiological parameters over the portion of the step included in the optimization, \bar{x}_{knee} , \bar{y}_{knee} , and $\bar{\theta}_{LL}$. The equation for computing the LLTE can, thus, be written as

$$\text{LLTE} = \sqrt{\frac{1}{N} \sum_{n=1}^N \left(\frac{x_n^{\text{knee}} - \hat{x}_n^{\text{knee}}}{\bar{x}_{\text{knee}}} \right)^2 + \left(\frac{y_n^{\text{knee}} - \hat{y}_n^{\text{knee}}}{\bar{y}_{\text{knee}}} \right)^2 + \left(\frac{\theta_n^{LL} - \hat{\theta}_n^{LL}}{\bar{\theta}^{LL}} \right)^2} \quad (1)$$

where n refers to the n th time interval and N is the total number of time interval considered in a step.

The design can then be optimized by selecting mechanical and geometric values that minimize the error between this trajectory and target physiological lower leg kinematics. This method was previously used to optimize simple analytical prosthetic foot models including (i) one with a pinned ankle and metatarsal joint,

Contributed by the Mechanisms and Robotics Committee of ASME for publication in the JOURNAL OF MECHANISMS AND ROBOTICS. Manuscript received September 15, 2017; final manuscript received December 28, 2017; published online March 2, 2018. Assoc. Editor: Andreas Mueller.

using constant rotational stiffnesses as design variables, and (ii) another with a pinned ankle joint and flexible forefoot, where rotational ankle stiffness and forefoot bending stiffness were the design variables [1].

Thus far, all work regarding LLTE has been purely theoretical. The next step in moving toward using the optimization metric to design commercial prosthetic limbs is to clinically test the validity of LLTE as a design objective for prosthetic feet. The goal of the present study was to create an experimental prosthetic foot to test the clinical viability of LLTE. The prototype prosthetic foot had to meet the following design requirements:

- Light enough that the weight of the foot does not affect the gait kinematics over the duration of the test.
- Fully mechanically characterized, such that the deformation of the foot under a given load can be calculated, thereby allowing evaluation of the LLTE value for the foot.
- Modular so that at least one design variable can be altered during testing in order to compare gait kinematics across a range of values of that design variable (e.g., ankle stiffness or forefoot bending stiffness).
- Able to express ankle stiffnesses greater or less than a physiological ankle while reaching physiological ranges of motion.

Our previous prototypes were built using commercially available steel coil springs. These feet proved to be too heavy and large and did not allow spring interchangeability [3,4]. The design presented in this study consists of a rotational ankle joint with interchangeable springs and a cantilever beam forefoot. The design variables of the architecture—the rotational stiffness of the ankle and the bending stiffness of the forefoot—were optimized using the LLTE. The considerations in building a physical prototype based on this theoretical design are discussed herein, and the resulting experimental device is presented. Our technique of using a constant moment spring to maximize strain energy storage and facilitate a high-stiffness, high-range of motion ankle may be of value to other researchers designing prosthetic feet. Mechanical testing results are included to show that the intended design specifications were satisfied. Qualitative feedback from preliminary user testing is also reported and discussed.

2 Lower Leg Trajectory Error Design Optimization Method

The conceptual architecture of the experimental foot consists of a rotational ankle joint with constant stiffness k_{ank} , and a flexible forefoot modeled as a cantilever beam with a stiffness k_{met} (Fig. 1), as presented in previous LLTE work [1,4]. The geometry of the rotational ankle, beam forefoot foot were selected to replicate the articulation of the physiological foot-ankle complex from a set of published gait data, with $h = 8.0$ cm and $d_{rigid} = 9.3$ cm [2]. The rigid structure length, d_{rigid} , was chosen such that the effective rotational joint of the pseudo-rigid-body model of the flexible forefoot during late stance would approximately coincide with the center of rotation of the metatarsal joint of a human foot. The pseudo-rigid-body model approximates a cantilever beam with a vertical end load as a rigid link and a rotational joint with stiffness related to the beam bending stiffness [5].

Values for the design variables, k_{ank} and k_{met} , were optimized in prior work using the LLTE design optimization method [1]. This method works by imposing physiological ground reaction forces (GRFs), matching the subjects' mass and size, on a model prosthetic foot with given stiffness and geometry. The resulting deflection, and thus the trajectory of the shank, can be computed and compared to physiological kinematics using the LLTE error function (Eq. (1)). The stiffness of the ankle and forefoot can then be tuned to reduce the LLTE [1]. For this study, Winter's gait data for a subject of body mass 56.7 kg [2] were used as inputs into the LLTE design optimization method. The set of design variables giving the lowest value for LLTE was taken to be the optimal

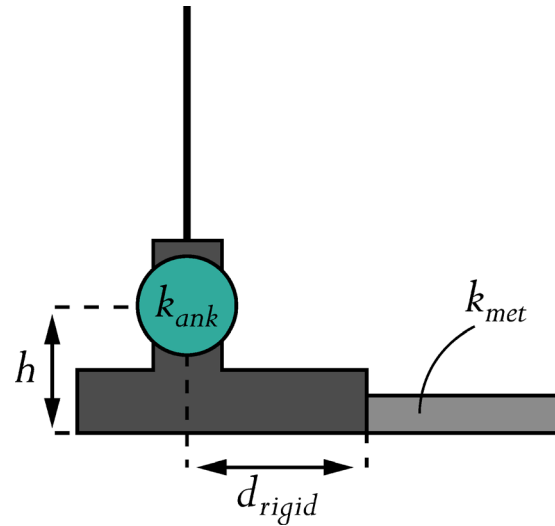


Fig. 1 Foot architecture, consisting of an ankle joint and a flexible forefoot modeled as a cantilevered beam. The position of the ankle joint and the forefoot have been chosen to replicate the articulation of the physiological foot-ankle complex.

design. The minimum LLTE value, 0.222, was calculated for $k_{ank} = 3.7$ N·m/deg and $k_{met} = 16.0$ N·m².

3 Mechanical Design of the Foot Experimental Device

In order to evaluate the LLTE as an optimization metric, it was necessary to design, build, and test prosthetic feet based on the optimal ankle and forefoot stiffnesses identified in Sec. 2. It is also important to understand the sensitivity of these stiffnesses on the foot's anticipated performance. Using the method presented by Olesnavage and Winter [1] and summarized in Secs. 1 and 2, the LLTE for this foot architecture (Fig. 1) was computed for each ankle and forefoot stiffness ranging from 0.5 N·m/deg to 25 N·m/deg and from 1 N·m² to 25 N·m², respectively. Figure 2 plots the LLTE for varying forefoot stiffnesses at the optimal ankle stiffness and for varying ankle stiffnesses at the optimal forefoot stiffness. It also shows that the LLTE value is much more sensitive to the ankle stiffness than the forefoot beam stiffness. We chose to fabricate five ankle stiffnesses that range from 1.5 to 24 N·m/deg to test in this study, which span an order of magnitude of LLTE values. Three stiffnesses were chosen at the optimum, slightly stiffer, and slightly less stiff. Two additional stiffnesses were chosen at much higher LLTE values, near the asymptotic limits, but still feasible to manufacture. The chosen range of ankle stiffnesses spans a similar range as ankle quasi-stiffness data from normal walking, which have been estimated as roughly 1.5–6.3 N·m/deg [6], 3.5–17.3 N·m/deg [7], or 3.5–24.4 N·m/deg [8] during different phases of gait.

It should be noted that the ankle and forefoot stiffness at the minimum LLTE value has the most physical relevance; this configuration of the foot would be most likely to replicate near-physiological kinematics and kinetics. An ideal foot with LLTE = 0 would facilitate a perfect replication. Since the LLTE is calculated using physiological GRFs as inputs, higher LLTE values (and thus higher predicted kinematic errors) indicate that some sort of compensation by a user of the foot would be likely. These compensations could manifest as modified kinematics or kinetics.

A solid model and the resulting physical prototype of this test foot are shown in Fig. 3. The rigid structural components were machined from acetal resin. The ankle joint rotates about a steel pin. Custom machined nylon 6/6 flexural springs fitted in aluminum mounts control the ankle joint rotational stiffness. The

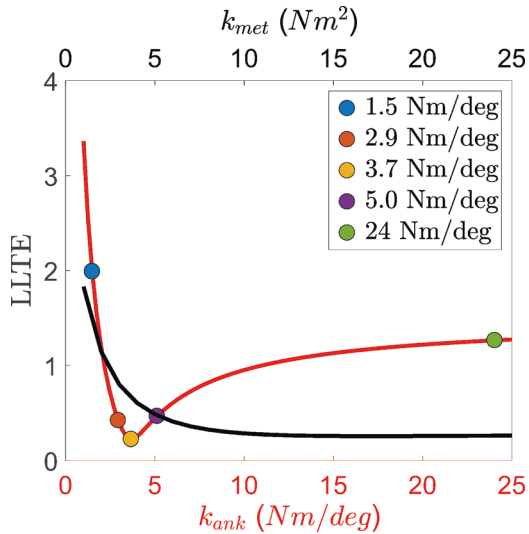


Fig. 2 Dependence of the LLTE value on the ankle stiffness k_{ank} and forefoot beam stiffness k_{met} . The sensitivity of the ankle rotational stiffness on the LLTE value for the optimal value of $k_{met} = 16.0 \text{ N} \cdot \text{m}^2$ is shown in red, and the sensitivity of the forefoot beam stiffness on the LLTE value for the optimal $k_{ank} = 3.7 \text{ N} \cdot \text{m}/\text{deg}$ is shown in black. The minimum LLTE value was achieved for $k_{ank} = 3.7 \text{ N} \cdot \text{m}/\text{deg}$ and $k_{met} = 16.0 \text{ N} \cdot \text{m}^2$. The five dots show the ankle stiffnesses selected to be fabricated as prototypes.

flexible forefoot was made from nylon 6/6 and was fixed to the rigid acetal resin structure with machine screws inserted into tapped holes in the acetal resin. As built, the experimental device has an average mass of 1.1 kg, which is approximately 52% less than the mass of our previous prototypes [3] and similar to the mass of a human foot, which is 1.45% of body weight [2] or 0.82 kg for a 56.7 kg person. The nylon springs were the critical design feature of the foot that facilitated the substantial mass reduction.

3.1 Spring Design Requirements. The entire foot mechanism needed to be compact and lightweight so that it did not interfere with gait and modular so that the ankle stiffness could be changed quickly by exchanging different springs. These requirements immediately precluded the use of commercially available coil springs, as existing coil springs of sufficient stiffness and range of motion were too heavy and bulky to allow interchangeability; therefore, custom springs were necessary. The custom springs had to withstand a moment of $105 \text{ N} \cdot \text{m}$ before yield, corresponding to the case in which a 56.7 kg user applies their body weight on the tip of the prosthesis toe. These loads required a material with a high yield strain ($\sigma_{yield} = \sigma_y/E$, where σ_y and E are the yield strength and elastic modulus of the material, respectively), and a high strain energy density ($u = (\sigma_y^2)/E$). Nylon 6/6 exhibited the best characteristics for a readily available, easy to machine material, with a strain energy density of 1.77 kJ/kg and a yield strain of 0.034 (McMaster-Carr, Inc, Elmhurst, IL). For the chosen ankle stiffness values (1.5, 2.9, 3.7, 5, and 24 N·m/deg (Fig. 2)), the ankle had to exhibit high ranges of motion, up to 30 deg, similar to biological ankles in order to replicate the expected lower leg trajectory.

3.2 Maximization of Strain Energy. The stiffness and range of motion requirements for the ankle spring exceeded the possible values for most common springs, even packaged leaf springs called flexural springs, which would commonly be used for a device of this size. Therefore, it was necessary to consider how to best maximize the strain energy stored in a spring. We chose a beam-type architecture for our springs for ease of manufacturing

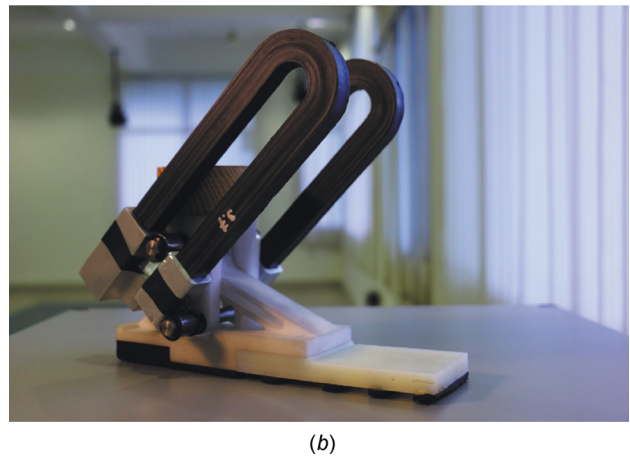
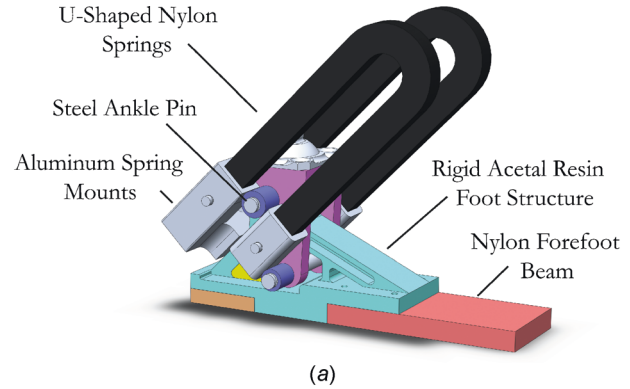


Fig. 3 Solid model (a) and photograph (b) of the prosthetic foot prototype with a constant rotational stiffness at the ankle of $k_{ank} = 3.7 \text{ N} \cdot \text{m}/\text{deg}$ and a forefoot beam stiffness of $k_{met} = 16.0 \text{ N} \cdot \text{m}^2$

and so the stiffness could be easily modified with geometric changes.

In a beam, the material will yield under a stress σ_y , corresponding to a maximum moment M_y applied to the beam. In a typical cantilevered beam bending scenario (Fig. 4(a)), the moment varies linearly from the tip to the base of the beam. The maximum moment, and thus the maximum strain energy stored per volume in the beam (for a constant cross section), occurs only at the base. The strain energy u is

$$u \sim \frac{\sigma^2}{E} \sim \frac{(My)^2}{EI^2} \quad (2)$$

where E is the modulus of elasticity, I is the area moment of inertia, and y is the distance from the neutral axis.

No strain energy is stored at the tip of the beam, and thus presents wasted strain energy storage potential. To maximize the strain energy stored in a beam of constant cross section, a uniform moment of M_y must be applied along the entire beam length. This can be achieved using a four-point beam bending scenario with rigid extremities (Fig. 4(b)). A beam loaded in this manner is able to store four times more elastic energy than a cantilevered beam of the same length and cross section.

3.3 Packaging and Fabrication. To package a constant moment beam in the prosthetic foot, the four-point beam was arranged into a U-shape (Fig. 5). This arrangement does not affect the force couple and moment reactions on each end of the beam, and to first-order estimates, retains a constant moment applied over the entire beam length. In our design, the U-springs springs

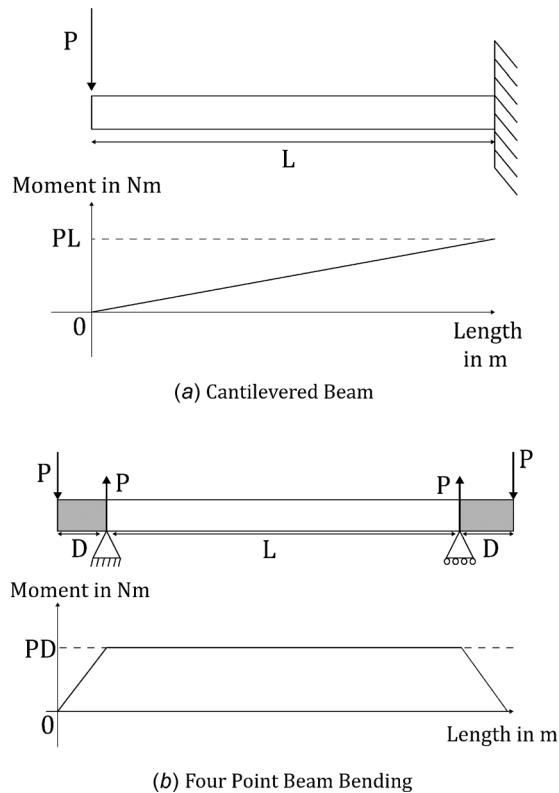


Fig. 4 Schematic of a beam of length L under a load P and the corresponding moment in the beam. For the four-point beam bending scenario (b), the moment arm length D corresponds to the beam length outside of the vertical supports.

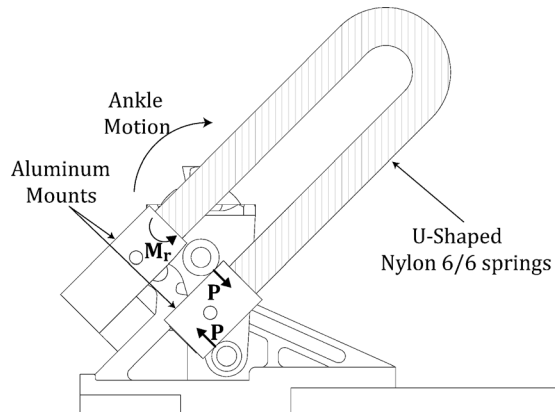


Fig. 5 Schematic of the U-shaped ankle spring under typical loading. P is the load applied to the beam (similar to the four point beam bending scenario in Fig. 4(b)) and M_r the reaction moment at the base.

are held by aluminum mounts that act as the rigid extremities and impose a rotation on the ends of the beam. These mounts also enable the springs to be easily exchanged. Changing the overall length and/or the width of the beam varies the rotational stiffness of the ankle.

First-order calculations were performed using Euler–Bernoulli beam bending theory to design the U-springs. A relation between the rotational stiffness of the beam (k_{beam}), its length (L), thickness (b), width (w), Young’s modulus (E), and yield stress (σ_y) was derived using Eqs. (3)–(5).

The maximum moment M_y under which the beam was loaded was derived from the yield stress of nylon 6/6 with a safety factor

of 1.2 (Eq. (3)). Then, the maximum end slope of the beam was calculated from M_y , the Young’s modulus of nylon 6/6, and the beam geometry (Eq. (4)). The end slope corresponded to half of the ankle angle θ_{ankle} , since in the ankle reference, one of the ends of the beam remains still. The rotational stiffness was then calculated as the moment divided by the ankle angle (Eq. (5))

$$M_y = \frac{2I\sigma_y}{b} \quad (3)$$

$$\theta_{\text{max}} = \frac{M_y L}{2EI} = \frac{\theta_{\text{ankle,max}}}{2} \quad (4)$$

$$k_{\text{ankle}} = \frac{M}{\theta_{\text{ankle}}} = \frac{Ewb^3}{12L} \quad (5)$$

Using Eqs. (3)–(5), a first estimate of the beam geometries was calculated to achieve the desired rotational stiffness with an applied moment of 105 N·m (corresponding to the case in which a 56.7 kg user applies their body weight on the tip of the prosthesis toe) before yield. Because the beam undergo large deformations and the radius of curvature of the beam at the curve is on the same order of magnitude as the thickness of the beam, the U-shaped beam is stiffer than a straight beam of the same length. Therefore, finite element analysis (FEA) was performed using the Solidworks simulation tool (Dassault Systemes, Inc, Vélizy-Villacoublay, France) to adjust the length of the U-shaped beam from the Euler–Bernoulli solution to achieve the desired rotational stiffness (Fig. 6). The U-shaped beam resulting from the finite element analysis was on average 60% shorter than the first-order estimate.

The U-shaped springs that yielded the optimal ankle stiffness of 3.7 N·m/deg had a thickness of 18.2 mm, a width of 14.0 mm, and a length of 160 mm. The length and width of the beams were varied to achieve the desired range of ankle stiffnesses (Fig. 7), which corresponded to those reported in Fig. 2. The total mass of a pair of nylon U-shaped springs was 80 g–400 g, with the optimal 3.7 N·m/deg springs weighing 225 g. The springs were mounted at an angle (Fig. 3), rather than vertically, to reduce the total foot volume and mass of the structure required to support them.

3.4 Cantilever Forefoot Design. The geometry of the beam forefoot was selected to replicate the articulation of the physiological foot [2] by placing the approximate rotational axis during bending (calculated from the pseudo-rigid body model) at the same location as the metatarsal joint [4]. A width w_b of 58.0 mm and a length l_b of 70.0 mm were chosen so that the total length of the foot was 21 cm. To achieve the beam bending stiffness of

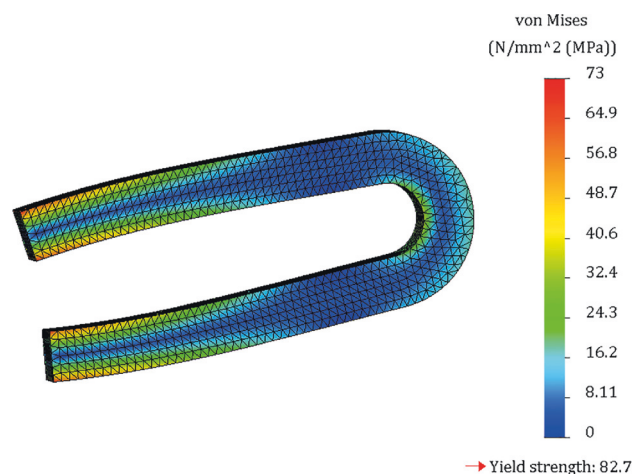


Fig. 6 FEA analysis of the U-shaped spring undergoing a moment of 52.5 N·m



Fig. 7 Set of springs with different rotational stiffness values. The longer the spring, the more compliant it is.

$k_{met} = 16.0 \text{ N} \cdot \text{m}^2$, several materials were considered such as acetal resin, nylon, polycarbonate, aluminum, and steel. The beam thickness h_b and maximum force (F_{max}) that can be applied to the tip of the beam were derived from their Young's modulus E and yield stress σ_y using the following equations:

$$k_{met} = \frac{E w_b h_b^3}{12} \quad (6)$$

$$F_{max} = \frac{\sigma_y h_b^2 w_b}{6 l_b} \quad (7)$$

From the desired stiffness values, nylon 6/6 could withstand the highest load before yielding. Thus, the beam forefoot was machined out of nylon 6/6 with a thickness $h_b = 11.1 \text{ mm}$, to achieve a bending stiffness $k_{met} = 16.0 \text{ N} \cdot \text{m}^2$ while withstanding a 612 N force, which corresponds to the maximum vertical GRF experienced during level ground walking [2] with a safety factor of 2.3.

3.5 Experimental Validation. The ankle rotational stiffnesses were measured using an Instron load testing machine (Universal Testing System, Instron, Illinois Tool Works, Inc, Norwood, MA). The experimental setup consisted of a jig constraining the test foot while the Instron loaded the rigid part of the forefoot, thus applying a moment on the ankle joint (Fig. 8). The Instron load cell was resistant to off-axis loading errors, with a force measurement error of 4.4% for this experiment. The foot was loaded at a constant rate of 300 mm/min until a moment of approximately 90 N·m on the ankle (corresponding to the maximum ankle moment experienced during flat ground walking from the Winter's data [2]) or the maximum ankle angle computed during the LLTE calculation of the specific ankle spring was

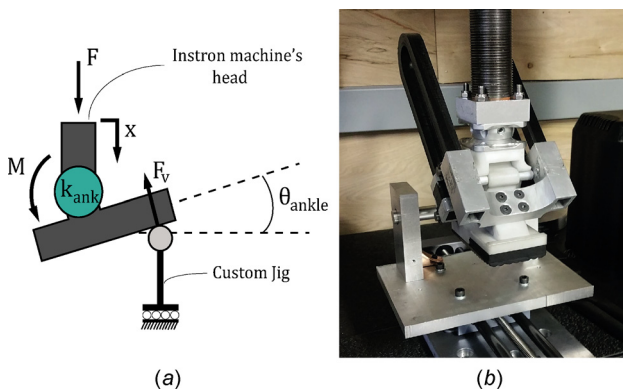


Fig. 8 Schematic of the experimental setup loading schematic (a) and photograph (b) of the prosthetic test foot being loaded on the Instron

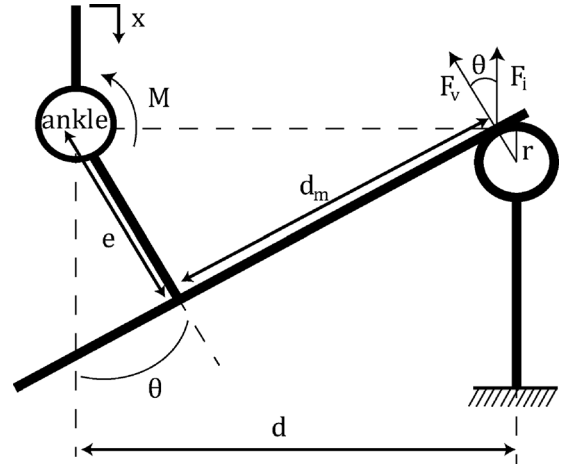


Fig. 9 Schematic of the geometric relations used to convert the collected load and displacement Instron data (x , F_i) into the ankle angle and moment data (M , θ)

achieved. The vertical load and displacement were recorded at a rate of 10 Hz.

The custom jig fixed on the Instron machine was composed of a linear stage on which an aluminum rod is mounted on a set of bearings. The foot is then loaded on the rigid part of the forefoot through the aluminum rod so that the load remains perpendicular to the foot at the contact point and the linear stage enables us to choose the exact position at which the vertical loads are applied.

The acetal foot structure on which the loads were applied was considered rigid in respect to the ankle springs since, under a moment of 90 N·m, the resulting deformation lead to an ankle angle error of 0.45 deg, which is negligible compared to the ankle spring range of motions tested here (5 deg–25 deg). The load and displacement data were then converted using geometric relations (Fig. 9) into ankle moment and angle data. Equation (8) was first solved to get the ankle angle θ , and then Eqs. (9) and (10) were used to compute the ankle moment M

$$\sin \theta (d - r \sin \theta - (e - x + r(1 - \cos \theta) \tan \theta)) = e - \frac{e - x + r(1 - \cos \theta)}{\cos \theta} \quad (8)$$

$$F_v \cos(\theta) = F_i \quad (9)$$

$$M = F_v d_m = F_i (d - r \sin \theta - (e - x + r(1 - \cos \theta) \tan \theta)) \quad (10)$$

The U-shaped springs all exhibited constant linear stiffnesses ranging from 1.5 to 24 N·m/deg, as desired. The U-spring experimental data are plotted in Fig. 10 showing rotational stiffnesses of 1.5, 2.9, 3.7, 5, and 24 N·m/deg. The linear fits of the experimental data agree with the finite element analysis for the rotational stiffness values with a 3% error and an average R^2 value of 0.994. The energy storage and return efficiency of these springs was on average 88% (Table 1). This reduced efficiency is most likely due to viscous flow in the material and friction losses at the ankle pin joint. The friction losses at the steel ankle pin (Fig. 3) were estimated on average to account for 26% of the total dissipated energy. The work done by dynamic friction (Eq. (11)) was computed using loading and angular data collected from the Instron, the steel pin radius $r_s = 4.8 \text{ mm}$ and, an acetal resin/steel dynamic coefficient of friction of $\mu_d = 0.3$ (Fig. 9)

$$W_{friction} \simeq \int \mu_d F_v r_s d\theta_{ankle} \quad (11)$$

The experimental testing of the foot presented earlier ensures accurate agreement between the stiffness values calculated with

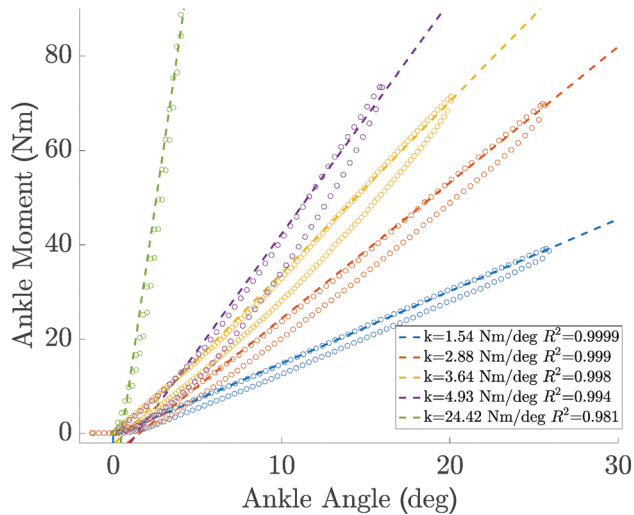


Fig. 10 Experimental data from testing the set of springs with corresponding rotational stiffness of 1.5, 2.9, 3.7, 5, and 24 N · m/deg are shown as circle markers. The dotted lines representing linear fits verifying the rotational stiffness value of the springs, which agree with the FEA-predicted values, are also shown. The springs showed some hysteresis due to viscous flow in the material.

Table 1 Ankle U-spring efficiencies, ratio between the stored and returned energy

Spring stiffness (N · m/deg)	1.54	2.88	3.64	4.93	24.4
Efficiency (%)	89.0	89.4	88.1	83.7	89.4

our LLTE design optimization method and the actual performance of the experimental prototype that will be used in clinical tests. The ankle stiffness ranged from 1.5 to 24 N · m/deg and exhibited ranges of motion of up to 30 deg. While the biological ankle also allows a 30 deg dorsiflexion of the foot [9], commercially available feet have a more limited range of motion. The SACH foot exhibits a 10 deg dorsiflexion for a stiffness of 16.3 N · m/deg [9,10], the rolling foot enables a 16 deg ankle range of motion for a stiffness of 3.8 N · m/deg [11], the seattle ankle/lite foot and the flex-foot allow a 20 deg dorsiflexion for an ankle stiffness of approximately 4.9 N · m/deg [9,10]. The designed experimental foot exhibited high ankle stiffnesses along with high ankle ranges of motion similar to those of a physiological foot and beyond those of common commercial products.

4 Preliminary Testing

The test foot was first tested using pseudo-prosthesis boots (Fig. 11) to ensure that both the compliant elements and the foot could withstand the typical loads experienced during flat-ground walking. The foot and different U-shaped springs were then tested on below-knee amputees in India (Fig. 12), who represent the target users of the high-performance, low-cost prosthetic limb technology we aim to produce through this research program. This study was approved of the MIT Committee on the Use of Humans as Experimental Subjects. The initial testing in India analyzed the comfort, functionality, spring interchangeability, reliability, and structural integrity of the foot to determine its suitability for use in clinical gait analysis studies and possible future clinical trials. The test foot was fitted on three male subjects with unilateral transtibial amputations who have been long-time users of the Jaipur foot, a common Indian prosthetic foot. The subjects had body masses ranging from 55 kg to 65 kg. Apart from the amputations,



Fig. 11 Pseudo-prosthesis boots mounted with the prosthetic foot prototype for preliminary testing



Fig. 12 Subject with below knee amputation testing the prototype at Bhagwan Mahaveer Viklang Sahayata Samiti, Jaipur

the subjects had no further pathologies. The subjects were asked to walk on flat ground using the prototype until they felt comfortable with it, at which point they were asked to walk up and down stairs and ramps.

Our prototype feet withstood several hours of testing on multiple subjects, using multiple ankle springs, and experienced no mechanical issues. The springs could be exchanged within a matter of minutes without removing the foot from the patient's prosthetic limb. The weight of the prosthesis was not a concern for the users and no additional issues were raised during testing. The subjects then completed a survey describing qualitatively what they liked and disliked about the prototype. Subjects liked the energy storage and return of the prototype and the increased walking speed. Dislikes were mainly focused on the aesthetics of the foot, which will be addressed in future iterations with cosmetic coverings. This positive feedback from preliminary testing was compelling enough to warrant further refinement of the foot design and its use for clinical studies.

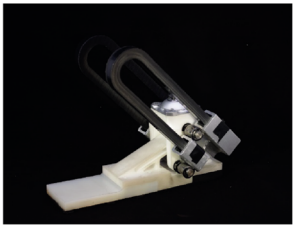
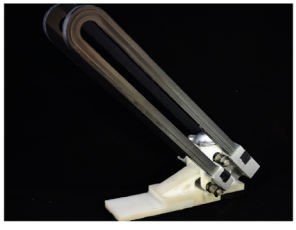
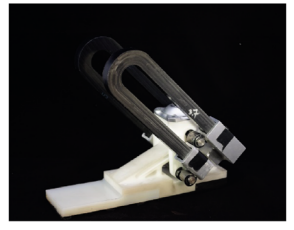
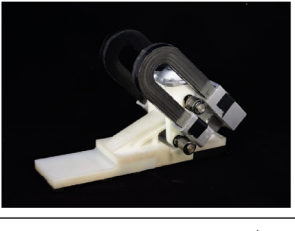
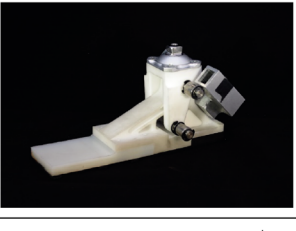
		
Ankle Stiffness : 1.54 Nm/deg Range of Motion: 30°	Ankle Stiffness : 2.88 Nm/deg Range of Motion: 30°	Ankle Stiffness : 3.64 Nm/deg Range of Motion: 30°
		Condition A: 1.54 Nm/deg Condition B: 2.88 Nm/deg Condition C: 3.64 Nm/deg Condition D: 4.93 Nm/deg Condition E: 24.4 Nm/deg
Ankle Stiffness : 4.93 Nm/deg Range of Motion: 25°	Ankle Stiffness : 24.4 Nm/deg Range of Motion: 6°	

Fig. 13 Photographs of tested prosthetic foot prototypes with ankle stiffness and range of motion values

5 In Vivo Testing

To further assess the mechanical behavior of the experimental prosthetic foot, in vivo testing was conducted at the Jesse Brown VA Medical Center Motion Analysis Research Laboratory in collaboration with the Northwestern University Prosthetics Orthotics Center. The foot was fitted to a transtibial subject who weighed 54.2 kg and measured 169 cm tall; this subject was chosen because her body mass and size was similar to that of the subject reported in Winter's gait data [2], which was used as inputs to our LLTE design optimization. The testing at Northwestern University Prosthetics Orthotics Center was performed according to the MIT Committee on the Use of Humans as Experimental Subjects approved protocol.

The subject tested each of the five ankle stiffnesses produced in this study. For each, she was asked to walk on flat ground using the prototype until she felt comfortable. After 10 min using the prototype, the subject walked at a comfortable, self-selected speed on the walkway, during which gait kinematic and kinetic data were recorded for at least five steps. The five different rotational ankle stiffness conditions tested (Fig. 13) are labeled A through E, where A is the most compliant spring and E is the stiffest. The ankle springs were changed on the prosthesis in a random order to avoid any biases from the subject. There was no need of any realignment between the socket and the foot since the foot remained firmly attached to the pylon during the entire process. The participant could rest as needed between each condition. Kinematic data were recorded through a motion capture system (Motion Analysis Corporation, Santa Rosa, CA), and kinetic data were measured by force plates (Advanced Mechanical Technology, Inc., Watertown, MA) embedded within the walkway. The entire set of data was then processed and analyzed through custom scripts implemented in MATLAB (The MathWorks, Inc, Natick, MA).

Stance phase ankle flexion moments and angles were computed from GRFs, center of pressure, and reflective marker position for each step and each stiffness condition. The measured in vivo ankle moment versus angle behavior were averaged over all steps for each condition and plotted against the mechanical testing data from Sec. 3.5 (Fig. 14). The in vivo test data align well with the mechanical behavior of the foot as measured on the Instron

material testing machine. During the controlled dorsiflexion phase of stance, the ankle angle–moment curves fit the Instron measurements with R^2 values of 0.73, 0.92, 0.82, 0.96, and 0.85 for conditions A through E, respectively. These results demonstrate that the analytical model of a purely rotational pin joint with a specified constant rotational stiffness used in this LLTE-based optimization adequately represented the actual in vivo mechanical behavior of the prosthetic foot prototype. Furthermore, the U-springs performed as desired in a clinical setting and did not adversely affect the subject's torque-angle ankle response.

However, the curvature in the in vivo test data does show that ankle springs exhibited larger hysteresis during terminal stance (unloading of the ankle springs) compared to the mechanical behavior of the foot as measured on the Instron machine. This is most likely due to viscoelastic effects of the nylon, as the

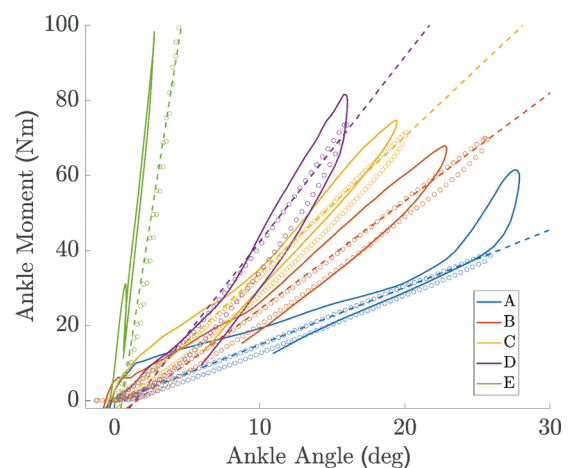


Fig. 14 Experimental data from testing the set of springs labeled condition A–E corresponding to rotational stiffnesses of 1.5, 2.9, 3.7, 5, and 24 N·m/deg are plotted in solid lines. Circle markers representing the Instron measured data and the dotted lines representing the expected ankle stiffness.

unloading rate in the in vivo testing was much higher than during the Instron testing.

6 Conclusions

This paper presents the physical design, mechanical characterization, preliminary user field testing, and in vivo stiffness measurements of a novel prosthetic foot architecture. The foot was able to accurately express stiffnesses calculated using our LLTE design optimization method, both in bench-top Instron and in vivo testing. These results are an important step in utilizing the LLTE optimization metric as a design tool to optimize prosthetic feet that can achieve desired kinematic and kinetic performance when worn by transtibial amputees.

The presented foot architecture enables rapid reconfiguration of different ankle stiffnesses and is able to provide ankle quasi-stiffness and range of motion values similar to those of a physiological foot and beyond those of common commercial products. The U-springs used in the ankle enable much higher strain energy density than could be obtained by cantilevered beams of the same length and volume. The presented spring design and foot architecture may be of value to other researchers who require high-stiffness and high-range of motion ankle joints.

Acknowledgment

Funding for this project was provided by the Tata Center for Technology and Design at MIT and the MIT Department of Mechanical Engineering. The authors would like to thank Mr. D. R. Mehta, Dr. Pooja Mukul, and Dr. M. K. Mathur at Bhagwan

Mahaveer Viklang Sahayata Samiti, the Jaipur Foot organization, and Rebecca Stine M.S. at Northwestern University for their continued support of this work.

References

- [1] Olesnavage, K. M., and Winter, A. G., 2015, "Lower Leg Trajectory Error: A Novel Optimization Parameter for Designing Passive Prosthetic Feet," IEEE International Conference on Rehabilitation Robotics (ICORR), Singapore, Aug. 11–14, pp. 271–276.
- [2] Winter, D. A., 2009, *Biomechanics and Motor Control of Human Movement*, 4th ed., Wiley, Hoboken, NJ.
- [3] Olesnavage, K. M., and Winter, A. G., 2015, "Design and Qualitative Testing of a Prosthetic Foot With Rotational Ankle and Metatarsals Joints to Mimic Physiological Roll-Over Shape," ASME Paper No. DETC2015-46518.
- [4] Olesnavage, K. M., and Winter, A. G., 2016, "Design and Preliminary Testing of a Prototype for Evaluating Lower Leg Trajectory Error as an Optimization Metric for Prosthetic Feet," ASME Paper No. DETC2016-60565.
- [5] Howell, L. L., 2001, *Compliant Mechanisms*, Wiley, New York.
- [6] Rouse, E. J., Hargrove, L. J., Perreault, E. J., and Kuiken, T. A., 2014, "Estimation of Human Ankle Impedance During the Stance Phase of Walking," *IEEE Trans. Neural Syst. Rehabil. Eng.*, **22**(4), pp. 870–878.
- [7] Shamaei, K., Sawicki, G. S., and Dollar, A. M., 2013, "Estimation of Quasi-Stiffness of the Human Hip in the Stance Phase of Walking," *PLoS One*, **8**(12), p. e81841.
- [8] Singer, E., Ishai, G., and Kimmel, E., 1995, "Parameter Estimation for a Prosthetic Ankle," *Ann. Biomed. Eng.*, **23**(5), pp. 691–696.
- [9] Wagner, J., Sienko, L. P. T. S. T., Supan, C. P. O. D., and Barth, C. P. O., 1987, "Motion Analysis of SACH Vs. Flex-Foot™ in Moderately Active Below-Knee Amputees," *Clin. Prosthet. Orthot.*, **11**(1), pp. 55–62.
- [10] Lehmann, J. F., Price, R., Boswell-Bessette, S., Dralle, A., Questad, K., and Quest, K., 1993, "Comprehensive Analysis of Dynamic Elastic Response Feet: Seattle Ankle/Lite Foot Versus SACH Foot," *Arch. Phys. Med. Rehabil.*, **74**(8), pp. 853–861.
- [11] Quesadag, P. M., Pitkin, M., Colvin, J., and Srinivasan, R., 2000, "Biomechanical Evaluation of a Prototype Foot/Ankle Prosthesis," *IEEE Trans. Rehabil. Eng.*, **8**(1), pp. 156–159.